A Mixed Oxidation State, Binuclear Iron Complex Containing an Unsymmetrically Coordinating Ligand. A Ligand-Induced Switch in Redox Behavior

Joe H. Satcher, Jr.,*[†,‡] Michael W. Droege,[†,§] Marilyn M. Olmstead,[‡] and Alan L. Balch*[‡]

Lawrence Livermore National Laboratory, Livermore, California 94550, and Department of Chemistry, University of California, Davis, California 95616

Received November 11, 1999

Binuclear $[Fe^{II}Fe^{III}(BMDP)(O_2CPh)_3](BF_4)$ **(1)** was obtained by treating an acetonitrile solution of the fully reduced $[Fe^{II}Fe^{II}(BMDP)(O_2CPh)(MeOH)_{1.5}(H_2O)_{0.5}](BF_4)_2$ with 5 equiv of benzoate and then exposing the mixture to oxygen. Examination of $[Fe^{II}Fe^{III}(BMDP)(O_2CPh)_3](BF_4)$ by X-ray crystallography reveals the localized, mixed oxidation state nature of the cation in the solid state. ^1H NMR and magnetic susceptibility data for the new complex are also reported. In the absence of dioxygen and other oxidants, treatment of $Fe^{II}Fe^{II}(BMDP)(O_2CPh)(MeOH)_{1.5}(H_2O)_{0.5}](BF_4)_2$ with excess benzoate results in the formation of $[Fe^{II}Fe^{II}(BMDP)(O_2CPh)_2](BF_4)_2$, which has also been characterized by X-ray diffraction.

Introduction

Redox active, binuclear iron centers in metalloproteins such as hemerythrin (Hr), ribonucleotide reductase (RR), methane monooxygenase (MMO), and purple acid phosphatase (PAP) are well established.[1−8] In these diiron proteins there is at least one mixed oxidation state ($Fe^{II}Fe^{III}$) form known. The metal centers in these metalloproteins also exist in an oxidized (Fe^{III}_2) form and with the exception of PAP, in a reduced (Fe^{II}_2) form. Hemerythrin (Hr) is considered the prototype for this class of proteins and has been shown crystallographically to contain an asymmetrically coordinated pair of Fe^{II} centers in its deoxy state.[9] One iron center is octahedrally bound to six donors: three nitrogen atoms from histidine residues, two oxygen atoms one each from two carboxylate residues (aspartate and glutamate), and a bridging hydroxo oxygen. The other iron center is bound to five donors: two nitrogen atoms from histidines, two oxygen atoms one each from two carboxylates, and the hydroxo oxygen bridge. On the basis of ^1H NMR solution experiments,[10] a trapped, mixed oxidation state ($Fe^{II}Fe^{III}$) configuration has been proposed for (semi-met)$_R$Hr. Subsequent interaction with dioxygen leads to an (Fe^{III}_2) form where proton migration from the hydroxo bridge results in a hydroperoxide ligand end-bound at the previously five coordinate iron center.[6,11,12]

The asymmetric nature of numerous binuclear metalloproteins and the ability of the metal ions to have quite distinct roles in the function of the enzyme are well-known.[13] We have approached the synthesis of models for these systems by using a binucleating ligand strategy incorporating an unsymmetrical multidentate chelate to mimic the coordination asymmetry.[13−17] For the case of unsymmetrical complexes resulting from the use of multidentate binucleating ligands with N and O donor atoms designed to induce coordination number asymmetry, the synthesis of such complexes has proven to be challenging, with only a few examples of binuclear iron complexes reported to date.[13] For example, Latour[18] et al. have synthesized a μ-phenoxo-bridged unsymmetrical mixed oxidation state ($Fe^{II}Fe^{III}$) complex, while Krebs[19] has successfully prepared an alkoxo-bridged fully oxidized (Fe^{III}_2) compound. We recently reported a reduced binuclear (Fe_2II) complex containing an alkoxo bridge and an unsymmetrical coordinating ligand.[16] Latour and coworkers also recently prepared an unsymmetrical ligand that provided iron coordination that included a single, terminally bound phenolate ligand.[20] The exchange of carboxylate and diphenylphosphate ligands has been examined within this asymmetric environment.[21] Here we report the structure and properties of an alkoxo-bridged, binuclear mixed oxidation state

---

* Authors to whom correspondence should be addressed.

[†] Lawrence Livermore National Laboratory.

[‡] University of California, Davis.

[§] Current address: Ocellus Inc., 2500 Saratoga St., Alameda, CA 94501.

(1) Feig, A. L.; Lippard, S. J. *Chem. Rev.* **1994**, *94*, 759.
(2) Que, L., Jr.; True, A. E. *Prog. Inorg. Chem.* **1990**, *38*, 97.
(3) Kurtz, D. M., Jr. *Chem. Rev.* **1990**, *90*, 585.
(4) Vincent, J. B.; Oliver-Lilley, G. L.; Averill, B. A. *Chem. Rev.* **1990**, *90*, 1447.
(5) Wilkins, R. G. *Chem. Soc. Rev.* **1992**, *21*, 171.
(6) Stenkamp, R. E. *Chem. Rev.* **1994**, *94*, 715.
(7) Nordlund, P.; Eklund, H. *J. Mol. Biol.* **1993**, *232*, 123.
(8) Wallar, B. J.; Lipscomb J. D. *Chem. Rev.* **1996**, *96*, 2625.
(9) Holmes, M. A.; Le Trong, I.; Turley, S.; Siecker, L. C.; Stenkamp, R. E. *J. Mol. Biol.* **1991**, *218*, 583.
(10) Maroney, M. J.; Kurtz, D. M., Jr.; Noeck, J. M.; Pearce, L. L.; Que, L., Jr. *J. Am. Chem. Soc.* **1986**, *108*, 6871.
(11) Stenkamp, R. E.; Sieker, L. C.; Jensen, L. H. *Proc Natl Acad Sci. U.S.A.* **1976**, *73*, 349.
(12) Stenkamp, R. E.; Sieker, L. C.; Jensen, L. H.; McCallum, J. D.; Sanders-Loehr, J. *Proc. Natl. Acad. Sci.* U.S.A. **1985**, *82*, 713.
(13) Fenton, D. E.; Okawa, H. *Chem. Ber./Recl.* **1997**, *130*, 433.
(14) Satcher, J. H., Jr.; Droege, M. W.; Weakley, T. J. R.; Taylor, R. T. *Inorg. Chem.* **1995**, *34*, 3317.
(15) Satcher, J. H., Jr.; Balch, A. L. *Inorg. Chem.* **1995**, *34*, 3371.
(16) Satcher, J. H., Jr.; Balch, A. L.; Olmstead, M. M.; Droege, M. W. *Inorg. Chem.* **1996**, *35*, 1749.
(17) Satcher, J. H., Jr.; Olmstead, M. M.; Droege, M. W.; Parkin, S. R.; Noll, B. C.; May, L.; Balch, A. L. *Inorg. Chem.* **1998**, *37*, 6751.
(18) Kanda, W.; Moneta, W.; Bardet, M.; Bernard, E.; Debaecker, N.; Laugier, J.; Boessoksou, A.; Chardon-Noblat, S.; Latour, J. M. *Angew. Chem., Int. Ed. Engl.* **1995**, *34*, 588.
(19) Euerling, B.; Schmidt, M.; Pinkernell, U.; Karst, U.; Krebs, B. *Angew. Chem., Int. Ed. Engl.* **1996**, *35*, 1973.
(20) Lambert, E.: Chabut, B.; Chardon-Noblat, S.; Deronzier, A.; Chottard, G.; Bousseksou, A.; Tuchagues, J.-P.; Laugier, J.; Bardet, M.; Latour, J.-M. *J. Am. Chem. Soc.* **1997**, *119*, 9424.
(21) Bernard, E.; Chardon-Noblat, S.; Deronzier, A.; Latour, J.-M. *Inorg. Chem.* **1999**, *38*, 190.

10.1021/ic9913177 CCC: $20.00

Table 1. Bond Lengths within Dinuclear Iron Complexes

$[Fe_2(BMDP)(O_2CPh)(MeOH)_{1.5}(H_2O)_{0.5}][BF_4]_2$ **(2)** (II,II), (6,5) $Fe^{II}1\ N_2O_4$, $Fe^{II}2\ N_3O_2$		$[Fe_2(BMDP)(O_2CPh)_2][BF_4]$ **(3)** (II,II), (5,5) $Fe^{II}1\ N_2O_3$, $Fe^{II}2\ N_3O_2$		$[Fe_2(BMDP)(O_2CPh)_3][BF_4]$ **(1)** (III,II), (6,6) $Fe^{III}2\ N_2O_4$, $Fe^{II}2\ N_3O_3$		
Fe(1)−O(1)	2.028(13)	Fe(1)−O(1)	1.993(4)	Fe(2)−O(1)	1.955(12)	alkoxo
Fe(1)−O(3)	2.081(12)	Fe(1)−O(3)	2.083(4)	Fe(2)−O(5)	1.950(13)	O_2CPh (bridging)
				Fe(2)−O(2)	2.002(14)	O_2CPh (bridging)
		Fe(1)−O(4)	2.024(4)	Fe(2)−O(6)	1.984(1)	O_2CPh (terminal)
Fe(1)−O(4)	2.152(17)					solvent
Fe(1)−O(5)	2.188(16)					solvent
Fe(1)−N(3)	2.140(18)	Fe(1)−N(4)	2.124(5)	Fe(2)−N(1)	2.143(16)	benzimidazole
Fe(1)−N(1)	2.327(18)	Fe(1)−N(2)	2.356(5)	Fe(2)−N(7)	2.258(14)	amine
Fe(2)−O(1)	1.968(10)	Fe(2)−O(1)	1.956(4)	Fe(1)−O(1)	2.042(11)	alkoxo
Fe(2)−O(2)	2.038(12)	Fe(2)−O(2)	2.054(4)	Fe(1)−O(4)	2.090(13)	O_2CPh (bridging)
				Fe(1)−O(3)	2.233(12)	O_2CPh (bridging)
Fe(2)−N(6)	2.106(14)	Fe(2)−N(6)	2.072(5)	Fe(1)−N(3)	2.169(16)	benzimidazole
Fe(2)−N(8)	2.078(16)	Fe(2)−N(8)	2.094(5)	Fe(1)−N(5)	2.131(19)	benzimidazole
Fe(2)−N(4)	2.299(16)	Fe(2)−N(1)	2.342(5)	Fe(1)−N(8)	2.312(17)	amine
Fe1···Fe2	3.556(6)	Fe1···Fe2	3.510(2)	Fe1···Fe2	3.454(6)	

($Fe^{II}Fe^{III}$) complex, which forms during the oxidation of the reduced unsymmetrical (Fe^{II}_2) precursor only when excess benzoate is present.[16]

Results and Discussion

$[Fe^{II}Fe^{III}(BMDP)(O_2CPh)_3](BF_4)$ **(1)** was obtained by treating an acetonitrile solution of the fully reduced $[Fe^{II}Fe^{II}(BMDP)(O_2CPh)(MeOH)_{1.5}(H_2O)_{0.5}](BF_4)_2$ **(2)**[16] with 5 equiv of sodium benzoate under a dinitrogen atmosphere. The resulting solution was then exposed to oxygen by bubbling air into the solution at room temperature to produce a clear, dark brown solution. Isolation of the product was effected by solvent diffusion of diethyl ether into the oxidized acetonitrile solution to yield golden-brown, prismatic crystals of **1** in ∼55% yield.

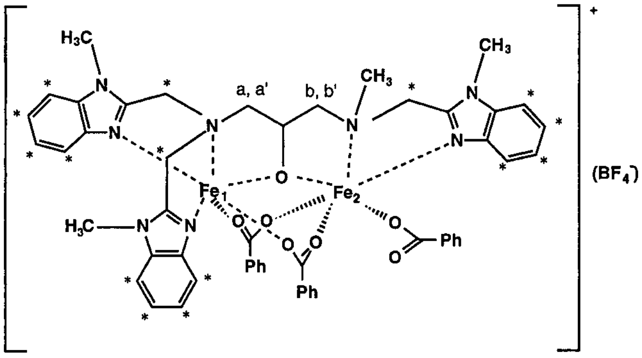

1, $[Fe^{II}Fe^{III}(BMDP)(O_2CPh)_3](BF_4)$

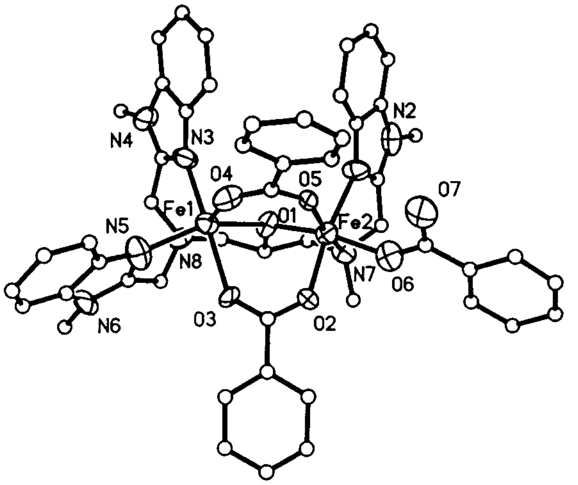

Figure 1. Structure of binuclear $Fe^{II}Fe^{III}$ cation, $[Fe^{II}Fe^{III}(BMDP)(O_2CPh)_3]^+$, with 25% thermal contours. Selected interatomic distances (Å): Fe1−O1, 2.042 (11); Fe1−O3, 2.233 (12); Fe1−O4, 2.090 (13); Fe1−N3, 2.169 (16); Fe1−N5, 2.131 (19); Fe1−N8, 2.312 (17); Fe2−O1, 1.955 (12); Fe2−O2, 2.002 (14); Fe2−O5, 1.950 (13); Fe2−O6, 1.984 (16); Fe2−N1, 2.143 (16); Fe2−N7, 2.258 (14); Fe1···Fe2, 3.454 (6).

As seen in Figure 1, the X-ray crystal structure of **1** reveals a central (μ-alkoxo)bis(μ-carboxylato) diiron core. As expected, the unsymmetrical ligand provides coordination asymmetry to the metal pair. However, in addition to the two bidentate bridging carboxylates, a monodentate carboxylate is also bound to Fe2 to produce pseudo-octahedral coordination about this center. The X-ray structural data for **1** is indicative of a mixed oxidation state complex. As seen in Table 1, there are significant differences in the in the Fe−O bond lengths for the two iron centers with average Fe−O distances and average deviations of 2.122(41) Å for Fe1 and 1.973(20) Å for Fe2. In particular the Fe1−O1−Fe2 bridge is unsymmetrical with the Fe1−O1 distance (2.042(11) Å) longer than the Fe2−O1 distance (1.955(12) Å). Thus, Fe1, with an N_3O_3 donor set, is assigned as the +II oxidation state, and Fe2 with an N_2O_4 donor set is assigned as the +III oxidation state. This donor set arrangement is opposite that found in the mixed oxidation state complex $[Fe^{II}Fe^{III}L^2(H_2O)(1,3\text{-benzenedipropionate})][BPh_4]_2$ in which the +II oxidation state metal center is located in the N_2O_4 environment and the +III metal is found with N_3O_3 coordination.[18] For comparison, the average Fe−O bond lengths found in the symmetrical mixed oxidation state complexes, $[Fe^{II}Fe^{III}$(2,6-bis-[(bis(2-pyridylmethyl)amino)methyl]-4-methylphenol)$(OPr)_2][BPh_4]_2$[22] and $[Fe^{II}Fe^{III}$(2,6-bis[(bis(1-methylimidazol-2-ylmethyl)-amino)methyl]-4-methylphenol)$(O_2CPh)_2][BPh_4]_2$[23], are 2.088 (2) and 2.107 (3) Å for Fe(II)-O, and 1.957 (2) and 1.973 (2) Å for Fe(III)-O, respectively. The Fe−Fe distance for **1** is 3.454 (6) Å, which is comparable to the 3.44 Å distanced found in semi-met hemerythrin azide by EXAFS.[24]

The magnetic properties of **1** in the solid state have been investigated at 1.0 kOe, over the temperature range 6−300 K.

---

(22) Borovik, A. S.; Papaefthymiou, V.; Taylor, L. F.; Anderson, O. P.; Que, L., Jr. *J. Am. Chem. Soc.* **1989**, *111*, 6183.

(23) Mashuta, M. S.; Webb, R. J.; McCusker, J. K.; Schmitt, E. A.; Oberhausen, K. J.; Richardson, J. F.; Buchanan, R. M.; Hendrickson, D. N. *J. Am. Chem. Soc.* **1992**, *114*, 3815.

(24) Scarrow, R. C.; Maroney, M. J.; Palmer, S. M.; Que, L., Jr.; Roe, A. L.; Salowe, S. P.; Stubbe, J. *J. Am. Chem. Soc.* **1987**, *109*, 7857.

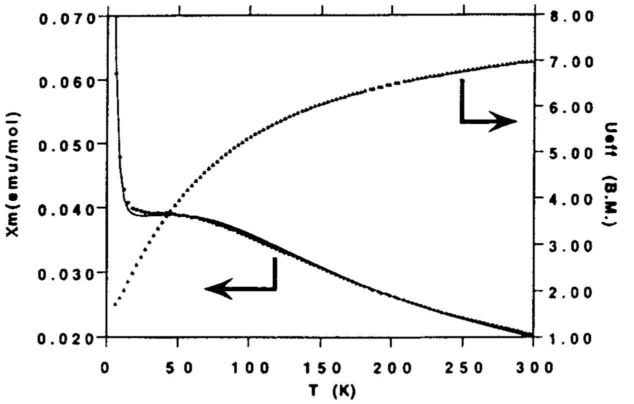

Figure 2. Temperature dependence of the corrected molar susceptibility and effective magnetic moment for $[Fe^{II}Fe^{III}(BMDP)(O_2CPh)_3][BF_4]$ (**1**) (6−300 K). The solid line is a least-squares fit of the molar susceptibility for all data. Final parameter set for fit assuming an isotropic g value: $2J = -8.8(1)$ cm^{-1}, $g = 2.0$ (fixed), t.i.p. 143×10^{-6} emu/mol.

The data are plotted as molar susceptibility (χ_{mol}) versus temperature in Figure 2. The effective moment per molecule at 300 K was found to be 7.03 μ_B for **1** in the solid state. On the basis of the crystal structure complex **1** was treated as a valence-localized system (i.e., class II in the Robin−Day scheme)[25] for calculating the magnetic exchange interaction. The temperature dependence of the susceptibility for **1** is thus given by the van Vleck eq 1. Here J is the intramolecular exchange interaction

$$\chi_M = Ng^2b^2f(J,T)/kT + \text{t.i.p.} \qquad (1)$$

in the Hamiltonian $H = -2JS_1 \cdot S_2$. The functions $f(J,T)$, which are tabulated elsewhere,[26] are weighted sums of exponentials e^{nx}, where n is an integer and $x = J/kT$. The data were successfully analyzed using a basis set with $S_1 = 2$ and $S_2 = {}^5/_2$ and yielded $2J = -8.8(1)$ cm^{-1}, $g = 2.0$ (fixed), and t.i.p. (temperature independent paramagnetism) $= 143 \times 10^{-6}$ emu/mol with a correlation $R = 0.99786$.[26−28] Inclusion of a monomeric impurity at a variable level did not improve the final fit.

The ^1H NMR spectra of **1** (and of **2** for comparison) in acetonitrile-d_3 at 23 °C are shown in Figure 3. The assignments of the resonances for **1** and **2** have been accomplished through consideration of relative peak areas and the use of selective deuteration.[29] (The proton sites indicated by asterisks in the drawing of **1** have been selectively deuterated.[16,29]) Several features of the spectrum of **1** indicate that the core features of the structure remain intact. The three benzimidazole methyl groups can be assigned by inspection of their peak areas. However, the aliphatic methyl group, which is found at 42.5 ppm in the spectrum of the (Fe^{II}_2) complex **2**, is not seen in the spectrum of the mixed oxidation state complex, **1**. This is presumably due to the interaction with the nearby paramagnetic Fe^{III} center (Fe2), which does not possess the favorable T_{1e} characteristics of the high-spin Fe^{II} oxidation state of Fe1.[30,31]

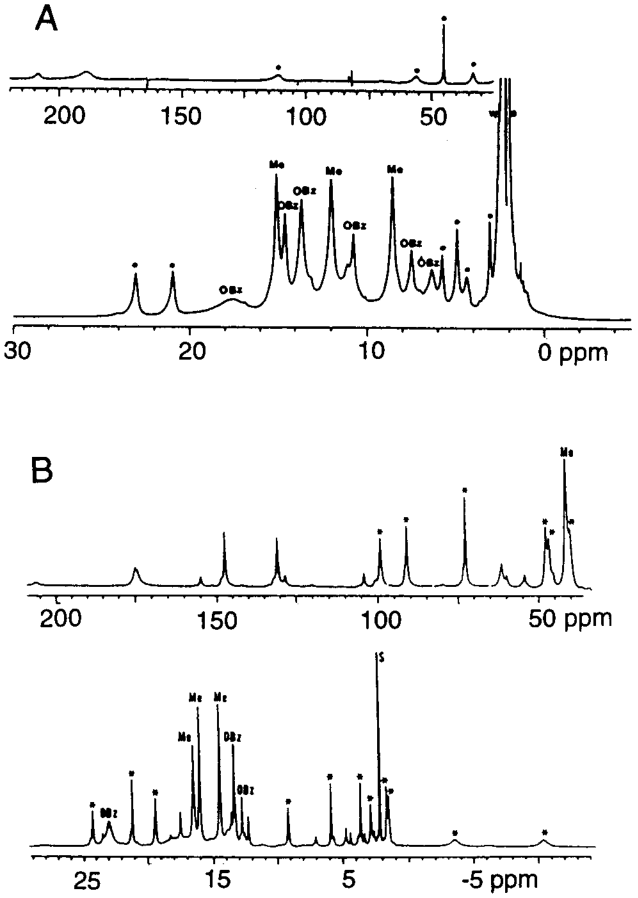

Figure 3. (A) The ^1H NMR spectrum (lower trace, −15 to 30 ppm; upper trace, 30 to 220 ppm) of **1**, $[Fe^{II}Fe^{III}(BMDP)(O_2CPh)_3][BF_4]$, in CD_3CN at 23 °C. (B) The ^1H NMR spectrum (lower trace, −15 to 30 ppm; upper trace, 30 to 220 ppm) of **2**, $[Fe^{II}Fe^{II}(BMDP)(O_2CPh)(MeOH)_{1.5}(H_2O)_{0.5}](BF_4)_2$, in CD_3CN at 23 °C. Peaks labeled with • or * are resonances that are removed on deuteration of the hydrogen atoms at locations denoted by asterisks in the drawing of **1**, s designates solvent resonance, OBz designates benzoate resonances, and Me designates methyl resonances.

Spectral observations of **1** using HBMDP-d_{18} and/or $[Et_3NH]O_2CPh$-d_5 allow the identification of the benzoate and aliphatic backbone peaks. The resonances of **1** at 210 and 188 ppm integrate to an intensity ration of 1:2 and are assigned as the sole methine and two of the methylene protons of the propanol backbone. A total area equivalent to 13 protons has been found for the benzoate groups, but the resonance(s) for the remaining two benzoate protons may be obscured by overlap or simply be broadened beyond detection. Peaks labeled with solid circles in Figure 3 are assigned to the hydrogen atoms at the positions in the drawing of **1** that are labeled with asterisks. Integration accounts for 11 of the possible 18 protons, and the remaining proton resonances again are presumed to be broadened beyond detection. These results are consistent with the solid state structure being preserved in solution and may suggest that the oxidation states of the two Fe ions in solution are localized on the NMR time scale. They also parallel observations found in the $[Fe^{II}Fe^{III}L^2(H_2O)(3\text{-benzenedipropionate})][BPh_4]_2$ system which also utilizes an unsymmetrical chelating ligand.[18] On the other hand, the symmetrical systems $[Fe^{II}Fe^{III}$(2,6-bis[(bis(2-pyridylmethyl)amino)methyl]-4-methylphenol)$(OPr)_2][BPh_4]_2$ and $[Fe^{II}Fe^{III}$(2,6-bis[(bis(1-methylimidazol-2-ylmethyl)amino)methyl]-4-methylphenol)$(O_2CPh)_2][BPh_4]_2$ (class III in the Robin−Day scheme) are reported to be valence delocalized in solution,[18,19] while $[Fe_2$(2-bis(salicylidineamino)methylphenol)$_2]^{2-}$,

---

(25) Robin, M. B.; Day, P. *Adv. Inorg. Chem. Radiochem.* **1967**, *10*, 247.
(26) O'Conner, C. J. *Prog. Inorg. Chem.* **1982**, *29*, 203.
(27) Carlin, R. L. *Magnetochemistry*; Springer-Verlag: Berlin, 1986; pp 2−4.
(28) Earnshaw, A. *Introduction to Magnetochemistry*; Academic Press: London, 1968; pp 4−8.
(29) Satcher, J. H., Jr. Ph.D. Thesis, University of California at Davis, December 1995.
(30) Bertini, I.; Turano, P.; Vila, A. J. *J. Chem. Rev.* **1993**, *93*, 2833.
(31) Bertini, I. Luchinat, C. *NMR of Paramagnetic Molecules in Biological Systems*; Benjamin/Cummins: Menlo Park, CA, 1986; p 137.

which is a class II complex in the Robin−Day scheme, has been shown to be valence delocalized in acetonitrile and dimethyl sulfoxide solutions.[32]

The ^1H NMR spectra of air-exposed acetonitrile solutions of the Fe^{II}_2 complex, **2,** in the presence of excess benzoate appear to consist solely of resonances of the mixed oxidation state complex **1**, and these samples are stable in air indefinitely. In addition, the isolated crystals of **1** are stable in air for weeks, and acetonitrile solutions prepared under nitrogen are stable for months. However, dissolution of **1** in acetonitrile-d_3 (no additional benzoate) in air leads to oxidation in which a fully oxidized iron species is slowly formed (∼1 h) based on the collapse of the range of the isotropically shifted resonances to the 0−50 ppm range and the observation of only broad ill-defined peaks. The unsymmetrical μ-phenoxo-bridged mixed oxidation state complex of Latour, however, is formed by reduction of an iron(III) species in solution and is air stable.[18] Toepler measurements of O_2 uptake for **2** (Fe^{II}_2) in acetonitrile show that one O_2 molecule is consumed per diferrous center. However, measurements of O_2 uptake for **2** in acetonitrile with additional benzoate show that one O_2 molecule is consumed by the *two* diferrous centers. The symmetric analogue of (Fe^{II}_2) **2**, the diferrous complex [Fe_2(*N*,*N*,*N′*,*N′*-tetrakis(2-(1-ethylbenzimidazoyl))-2-hydroxy-1,3-diaminopropane)(O_2CPh)][BF_4]$_2$, has been reported to combine with 1 mol of O_2 per iron pair.[33] A metastable *cis*-μ-1,2 peroxo-bridged diiron complex of that ligand has been successfully isolated and crystallographically characterized by Que and co-workers.[34] However, we have observed that addition of excess benzoate to a solution of this symmetric analogue of **2**, followed by exposure to air, leads directly to a fully oxidized complex at room temperature (as determined by ^1H NMR) without an isolable mixed oxidation state complex.

The mixed oxidation state complex **1** can thus be considered as an "arrested" oxidation state complex in which excess benzoate is used as a switch to inhibit complete oxidation. Clearly additional benzoate is required by stoichiometric considerations to form **1** from **2**, but others factors such as charge compensation and tuning of redox potentials are also likely to play a role in governing the formation of **1** during oxidation. It remains to be seen whether other ligands can also be used to stabilize other mixed oxidation state complexes analogous to **1**.

In the absence of dioxygen, addition of excess sodium benzoate to $[Fe^{II}Fe^{II}(BMDP)(O_2CPh)(MeOH)_{1.5}(H_2O)_{0.5}](BF_4)_2$ **(2)**[16] under a dinitrogen atmosphere leads to the formation of **3**, $[Fe^{II}_2(BMDP)(O_2CPh)_2][BF_4]\cdot 2CH_3OH$. As seen in Figure 4, the X-ray crystal structure of **3** reveals a central (μ-alkoxo)-bis(μ-carboxylato) diiron core with a bridging benzoate ligand. Structural parameters for the cation are given in Table 1. The other benzoate ligand is bound to iron in a monodentate fashion. As expected, the unsymmetrical ligand again provides coordination asymmetry to the metal pair. In the cation **3**, Fe2 is five-coordinate with distorted trigonal bipyramidal geometry. An amine nitrogen atom and a benzoate oxygen atom occupy the axial positions. The other iron atom, Fe1, is also five-coordinate with a distorted square pyramidal geometry. A benzimidazole nitrogen atom occupies the apical position while the amine nitrogen atom, two benzoate oxygen atoms, and the alkoxo oxygen atom reside in the basal plane sites.

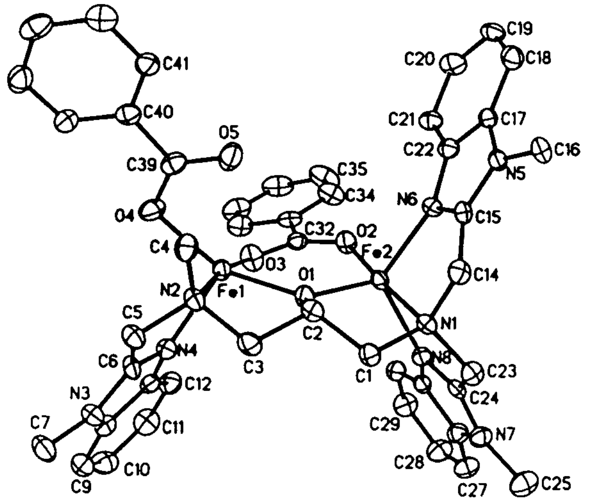

Figure 4. Structure of binuclear $Fe^{II}Fe^{II}$ cation, $[Fe^{II}_2(BMDP)(O_2CPh)_2]^+$, with 25% thermal contours.

Experimental Section

Preparation of $[Fe^{II}Fe^{III}(BMDP)(O_2CPh)_3][BF_4]$ (1). A solution of 0.0200 g (0.0212 mmol) of $[Fe_2(BMDP)(O_2CPh)(MeOH)_{1.5}(H_2O)_{0.5}][BF_4]_2$ **(2)**[16] in 0.75 mL of acetonitrile was treated with an acetonitrile solution (0.75 mL) containing 0.0130 g of benzoic acid (0.106 mmol) and 0.0107 g of triethylamine (0.106 mmol) with stirring under a dinitrogen atmosphere. The light yellow solution was exposed to oxygen by bubbling 3 cm^3 of air into the tube. The resulting brown solution was layered with diethyl ether, and the tube was capped with a rubber septum. After 4 days, the crystalline solid was collected on a glass frit, washed with 2 × 3 mL portions of ether, and vacuum-dried at ambient temperature to yield 0.0128 g of golden brown crystals (55.1% yield). IR (KBr cm^{-1}): ν_{asym}(COO) 1600; ν_{sym}(COO) 1559; n(BF_4) 1054.

Preparation of $[Fe^{II}_2(BMDP)(O_2CPh)_2][BF_4]\cdot 2CH_3OH$ (3). Diffraction quality crystals were prepared by diffusion of diethyl ether into a methanol solution of $[Fe_2(BMDP)(O_2CPh)(MeOH)_{1.5}(H_2O)_{0.5}][BF_4]_2$ to which 5 equiv of sodium benzoate had been added. Pale yellow crystals were formed on standing. Alternately, the complex could be obtained by adding a solution of 0.200 g (0.346 mmol) of HBMDP and 0.250 g of sodium benzoate in 4 mL of methanol to a solution of 0.236 g of $Fe(BF_4)_2\cdot 6H_2O$ in 4 mL of methanol under an atmosphere of dioxygen-free dinitrogen. The light yellow solution that formed was filtered and allowed to slowly evaporate under dinitrogen. The pale yellow crystalline solid was collected by filtration, washed with 2 × 1 mL portions of methanol, and vacuum-dried at ambient temperature to give 0.235 g (64%) of the product.

X-ray Crystallography for $[Fe^{II}Fe^{III}(BMDP)(O_2CPh)_3][BF_4]$ (1). The crystal selected for data collection was mounted in the cold stream (125 K) of a Siemens P4 diffractometer equipped with an LT-2 low-temperature apparatus. The radiation employed was Ni filtered Cu Kα from a Siemens rotating anode source operating at 15 kW. The data were collected using $2\theta-\omega$ scans from 0° to 110.0° at 8° min^{-1}. Values of neutral atom scattering factors, f' and f'', and absorption coefficients were taken from a standard source.[35]

Crystal data for **1** ($C_{52}H_{50}BF_4Fe_2N_8O_7$, MW = 1097.5) at 125 K: golden brown prisms, orthorhombic, space group $P2_12_12_1$, $a = 14.181(2)$ Å, $b = 18.883(4)$ Å, $c = 19.008$ (4) Å, $V = 5090(2)$ Å^3, $Z = 4$. A total of 3587 unique reflections were collected.

The structure was solved using direct methods. Hydrogen atoms were added geometrically and refined by use of a riding model and an isotropic thermal parameter equal to 1.2 times the equivalent isotropic thermal parameter of the bonded carbon atom. Distance restraints were applied to the fluoroborate anion to aid convergence. An absorption correction (XABS), which provides an empirical correction for absorp-

---

[32] Snyder, B. S.; Patterson, G. S.; Abrahamson, A. J.; Holm, R. H. *J. Am. Chem. Soc.* **1989**, *111*, 5214.

[33] Dong, Y.; Ménage, S.; Brennan, B. A.; Elgren, T. E.; Jang, H. G.; Pearce, L. L.; Que, L., Jr. *J. Am. Chem. Soc.* **1993**, *115*, 1851.

[34] Dong, Y.; Yan, S.; Young, V. G., Jr.; Que, L., Jr. *Angew. Chem., Int. Ed. Engl.* **1996**, *35*, 618.

tion based on F_o and F_c differences, was applied.[36] Refinement was accomplished by full-matrix least-squares methods, based on F^2, using all 3587 data and 643 parameters to obtain final indices $R = 0.0913$ for 2186 data with $I > 2\sigma(I)$ and wR2 = 0.2699 for all 3587 data. Anisotropic thermal parameters were used only for the non-hydrogen atoms of the cation. The largest peak in the final difference map had height of 0.51 e Å^{-3} and is 0.85 Å from F1.

X-ray Crystallography for [Fe$^{II}_2$(BMDP)(O$_2$CPh)$_2$][BF$_4$]·2CH$_3$OH (3). The crystal selected for data collection was mounted in the cold stream (125 K) of a Siemens R3m/V diffractometer equipped with a locally modified Nonius low-temperature apparatus. The radiation employed was graphite-monochromated Mo Kα. The data were collected using ω scans from 0° to 45° at 8.08° min^{-1} in ω.

Crystal data for **3** ($C_{47}H_{53}BF_4Fe_2N_8O_7$, MW = 1040.48) at 125 K: golden-brown prisms, triclinic, space group $P\bar{1}$, $a = 11.527(4)$ Å, $b = 11.753(4)$ Å, $c = 20.570(6)$ Å, $\alpha = 78.56\ (2)°$, $\beta = 74.60(2)°$, $\gamma = 81.84(3)°$, $V = 2621.5(14)$ Å^3, $Z = 2$. A total of 9160 unique reflections were collected.

Calculations were performed using the SHELXS-97 and SHELXL-97 program system. The structure was solved using direct methods. Values of neutral atom scattering factors, $f\,'$ and $f\,''$, and absorption coefficients were taken from a standard source.[35] Hydrogen atoms were added geometrically and refined by use of a riding model and a fixed isotropic thermal parameter of 0.08 Å^2. Distance restraints were applied to the tetrafluoroborate anion to aid convergence. There is disorder in the positions of the fluorine atoms of the tetrafluoroborate anion which were found to occur in two orientations. These were modeled with variable occupancy and rigid body restraints. Site A had a refined occupancy of 0.564(12) while site B had an occupancy of 0.436(12). Several sites were partially occupied by molecules of methanol. Two sites were assigned 0.50 occupancy while three others were refined with 0.33 occupancy. No absorption correction was performed.

Refinement was accomplished by full-matrix least-squares methods, based on F^2, and produced a final wR2 value of 0.244. A conventional R1 = 0.080 was calculated using 5820 observed ($I > 2\sigma$(I)) data, 620 parameters, and 25 restraints. Anisotropic thermal parameters were used for all non-hydrogen atoms of the cation. The largest peak in the final difference map had a height of 1.20 e Å^{-3} and is in the vicinty of C(91).

Magnetic Susceptibility Studies. Magnetic susceptibility measurements were obtained at an applied field of 1 kOe on a Quantum Design SQUID magnetometer operating between 6 and 300 K. Measurement of the magnetic moment at 6 K as a function of field between 0.1 and 55 kOe demonstrated the lack of saturation effects. Determinations were made on finely ground crystalline samples loaded into gelatin capsules. Diamagnetic corrections for the capsules were made by direct measurement, while correction for the ligand HBMDP was calculated by use of Pascal's constants.[26−28] Calibration of the instrument was performed using HgCo(SCN)$_4$.[26]

Acknowledgment. We are grateful to the Gas Research Institute (GRI), Department of Energy, Morgantown Energy and Technology Center (DOE-METC), and the Lawrence Livermore National Laboratory, Institutional Research and Development Program (LLNL Directors Initiative), for their generous support. Work performed under the auspices of the US Department of Energy by the Lawrence Livermore National Laboratory under contract No. W-7405-ENG-48.

Supporting Information Available: For complexes **1** and **3**, full tables of structural parameters and refinement data, atom coordinates, bond distances and angles, and anisotropic thermal parameters. Crystallographic data in CIF format. This material is available free of charge via the Internet at http://pubs.acs.org.

IC9913177

---

(35) *International Tables for Crystallography*; Wilson, A. J. C.; Kluwer Academic Publishers: Dordrecht, 1992; Vol. C.

(36) Parkin, S. R.; Moezzi, B.; Hope, H. *J. Appl. Crystallogr.* **1995**, *28*, 53.